Eur. J. Mech., A/Solids, **17**, n° 2, 185-205, 1998

Thermodynamics of isotropic pseudoelasticity in shape memory alloys

B. RANIECKI * and CH. LEXCELLENT **

ABSTRACT. – The thermodynamic theory of the pseudoelastic behaviour of SMA is generalized to include new observed effects in isotropic solids. It has been shown that macroscopic eigenstrain due to martensitic phase transitions (p.t.) is a homogeneous function of the stress of order zero, provided that partial thermodynamic equilibrium occurs. The specific form of the Gibbs potential is presented and new conditions for the initiation of p.t. are derived. They are expressed in terms of the temperature, second and third invariants of the stress deviator. The thermostatic properties and phenomenological constants are found for a NiTi alloy using experimental data reported in the literature. The theoretical and experimental results are compared for simple tension compression and pure shear. © Elsevier, Paris

Notation

$$trA = A_{ii};\ \boldsymbol{A}\cdot\boldsymbol{B} = A_{ij}B_{ij};\ \boldsymbol{AB} \rightarrow A_{ijmn}B_{mn},\ 1 \rightarrow \delta_{ij}\ \text{(Kronecker's symbol)}$$

1. Introduction

In order to account for the essence of behaviour of shape memory alloys (SMA) including stress-strain-temperature coupling a thermodynamically consistent formulation is necessary. The details of energetic description of pseudoelastic behaviour of SMA may be found in recent papers (Müller, 1989), (Müller and Xu, 1991), (Raniecki *et al.*, 1992), (Huo and Müller, 1993), (Sun and Hwang, 1993), (Raniecki and Lexcellent, 1994), (Jesse Lim and McDowell, 1995), (Leclercq and Lexcellent, 1996) and (Boyd and Lagoudas, 1996) which use the framework of thermodynamics of irreversible processes to incorporate experimentally observed main features of the SMA behaviour. The present authors (R and L, 1994) and (R *et al.*, 1992) have developed the class of so called R_L - models that are able, e.g., to incorporate most of the basic features of formation of pseudoelastic hysteresis loops observed by (H and M, 1993) in uniaxial situation. The models are valid for complex stress state and they employ versatile phase transition kinetics relations including not only ideal but also nonlinear pseudoelastic

---

* Institute of Fundamental Technological Research, Polish Academy of Sciences, Świetokrzyska 21, 00-049 Warsaw, Poland.

** Laboratoire de Mécanique Appliquée, Raymond Chaléat, UMR CNRS 6604, UFR Sciences, 25030 Besançon Cedex, France.

EUROPEAN JOURNAL OF MECHANICS, A/SOLIDS, VOL. 17, N° 2, 1998
0997-7538/98/02/© Elsevier, Paris

flow. They predict the existence of two limiting surfaces in stress space for pseudoelastic flows associated with forward and reverse stress-induced phase transitions (p.t.). The recently reported experimental results (*cf.* Sittner and Tokuda, 1994 and Rogueda *et al.*, 1996) obtained under two-parameter (torsion-tension) proportional loadings seem to confirm those predictions. However, the experimental observations indicate the important deviations of the shape of actual limiting surfaces from the spheres discussed in (R *et al.*, 1992) and (R and L, 1994). The experiments (Roumagnac, 1993, R *et al.*, 1996, Vacher and Lexcellent, 1991 and Orgeas and Favier, 1996) also show the substantial discrepancy between the pseudoelastic limits in tension and compression. More particularly, (O and F, 1996) notified the following experimental observations:

a) The critical stress for forward p.t. in tension (limit of pseudoelastic flow) σ_T^{AM} is smaller than the absolute value of corresponding critical stress $\sigma_C^{AM} < 0$ in compression, i.e., $\sigma_T^{AM} < -\sigma_C^{AM}$.

b) The pseudoelastic amplitude γ_T in tension is greater than the one found in compression, say γ_C. However, the energies in tension and compression represented by product of critical stress (for forward p.t.) and pseudoelastic amplitude are the same, i.e.,

$$\gamma_T > \gamma_C, \qquad \sigma_T^{AM}\gamma_T = \gamma_C|\sigma_C^{AM}| = \mathbb{C}(T)$$

where T is the temperature.

c) Both σ_T^{AM} and σ_C^{AM} are linear functions of the temperature. However, the temperature-sensitivity of pseudoelastic limit is greater in compression than in tension, i.e.,

$$-\frac{d\sigma_C^{AM}}{dT} > \frac{d\sigma_T^{AM}}{dT}$$

d) The hysteresis width obtained in compression is greater than the one measured in tension.

e) The observed behaviour in pure shear is symmetric.

Although most of recently proposed thermodynamical models have used some of fundamental issues of the micromechanics they are not expected to reproduce the strong tensile-compressive asymmetry and other aforementioned effects without special modifications. The R_L-models seem to be the only 3-D phenomenological models employing the concept of thermodynamical instability which originates the martensitic phase transformations. They are the simplest workable models which were successfully applied e.g., in the designing of bronchial prosthesis (Leclercq *et al.*, 1996), in the analysis of the efficiency of a solid state engine (Źiółkowski, 1993) and in the analysis of coupled effects occurring during pseudoelastic deformations (Źiółkowski and Raniecki, 1996). However, they are applicable only in the temperature range where pseudoelasticity of SMA is observed ($T > A_f^0$).

The main objective of the present paper is to develop generalized thermostatics consistent with (R and L, 1992) which account for all experimental trends (a)-(e) observed by (O and F, 1996).

2. Basic concepts of thermostatic of pseudoelasticity

2.1. FORMS OF THERMODYNAMIC POTENTIALS

Consider a piece of SMA (representative macroscopic volume element - RVE) which at a reference state (stress $\boldsymbol{\sigma} = 0$, temperature $T = T_0$) is the single phase solid. This phase will conventionally be referred to as "austenite" (A), and it will be regarded as a high-temperature phase. Its properties will be denoted by index $\alpha = 1$. Under applied thermomechanical loading, austenite can be transformed ("forward" p.t.) into low-temperature phase called "martensite" (M). The properties of martensite will be denoted by index $\alpha = 2$. Under appropriate loading paths, martensite can be transformed back into the initial phase A, and such process is termed "reverse" p. t. $M \rightarrow A$. Suppose that a non-equilibrium state of two-phase RVE is described by:

ε_α – total intrinsic strains of phases $(\alpha = 1, 2)$,

T – actual temperature,

z – volume fraction of martensite

h_K – a set of internal variables $(K = 1, 2 \ldots)$.

We do not specify the number and the physical character of h_K. The basic conclusions derived in this paper will not depend on this information. In general h_K are variables of displacement type. They are supposed to represent actual rearrangements of the internal pattern observed in the RVE on microscale, e.g., the change in mutual orientations of martensite active systems.

Consider the following form of the specific free energy Φ_n for a two-phase mixture [R *et al.*, 1992],

$$(1) \qquad \Phi_n = \Phi_n(T, \varepsilon_\alpha, z, \boldsymbol{h}) = (1-z)\phi^{(1)} + z\phi^{(2)} + \phi_{it} z(1-z); \qquad \phi_{it} = \bar{u}_0 - T\bar{s}_0$$

where ϕ_{it} ($\bar{u}_0$, $\bar{s}_0$ are constants) represents type of configurational energy associated with the coherency of phases (R and L, 1994; H and M, 1993). Both phases are regarded as thermoelastic solids that have equal temperature independent thermoelastic constants $\boldsymbol{L}$ – elastic moduli, $\boldsymbol{\alpha}$ - thermal expansion coefficients and c_p – specific heat at constant stress) such that $(\alpha = 1, 2)$,

$$(2) \qquad \phi^\alpha = \overset{*}{u}{}_0^\alpha - T\overset{*}{s}{}_0^\alpha + c_p[T - T_0 - T\ln(T/T_0)] + (\varepsilon_\alpha - \varepsilon_\alpha^f) \cdot \boldsymbol{L}(\varepsilon_\alpha - \varepsilon_\alpha^f)/2\rho$$

where mass density of austenite ρ, internal energies $\overset{*}{u}{}_0^\alpha$ and entropies $\overset{*}{s}{}_0^\alpha$ of individual phases $(\alpha = 1, 2)$, at reference state, are treated as constants.
Moreover, $\varepsilon_{(1)}^f = \boldsymbol{\alpha}\Delta T$, $\Delta T = T - T_0$,

$$(3) \qquad \varepsilon_{(2)}^f = \boldsymbol{\kappa}(\boldsymbol{h}) + \boldsymbol{\alpha}\Delta T$$

where $\boldsymbol{\kappa}$ is the traceless $(tr\boldsymbol{\kappa} = 0)$ eigenstrain associated with the formation of the martensite phase. Thus, it is stipulated that merely eigenstrain $\boldsymbol{\kappa}$ depends on internal variables h_K. In general, $\overset{*}{u}{}_0^{(2)}$ and ϕ_{it} are also influenced by microstructural changes. Here, however, effects of such variations are neglected.

Denote by ε the total overall strain of the two-phase RVE. Under prescribed ε, the intrinsic strains ε_α must satisfy the following constraint relation

$$\varepsilon = (1-z)\varepsilon_{(1)} + z\varepsilon_{(2)} \tag{4}$$

One assumes that during the actual process of straining, the macroelement is in mechanical equilibrium, i.e., that the free energy function (1) reaches the constrained minimum with respect to the variables ε_α at fixed ε, T, z and h_K. Using (1) and (4), it can be shown (R *et al.*, 1992) that in mechanical equilibrium, the intrinsic phase stresses defined by $\boldsymbol{\sigma}_\alpha = \rho\partial\phi^\alpha/\partial\varepsilon_\alpha$ are equal to the overall macroscopic stress $\boldsymbol{\sigma}$. From this condition, one can determine the equilibrium values of ε_α,

$$\varepsilon_{(1)}^{eq} = \varepsilon - z\boldsymbol{\kappa}(\boldsymbol{h}); \qquad \varepsilon_{(2)}^{eq} = \varepsilon + (1-z)\boldsymbol{\kappa}(\boldsymbol{h}) \tag{5}$$

Inserting (5) into (1) one finds the following function of the free energy

$$\begin{aligned}\Phi'_{eq}(T,\varepsilon,z,\boldsymbol{h}) = \Phi_n\,|_{\varepsilon_\alpha=\varepsilon_\alpha^{eq}} &= \overset{*}{u}{}_0^{(1)} - T\overset{*}{s}{}_0^{(1)} - z\pi_0^f(T)\\ &+ c_p[\Delta T - T\ln(T/T_0)] + z(1-z)\phi_{it}\\ &+ [\varepsilon - z\boldsymbol{\kappa}(\boldsymbol{h}) - \boldsymbol{\alpha}\Delta T]\cdot\boldsymbol{L}[\varepsilon - z\boldsymbol{\kappa}(\boldsymbol{h}) - \boldsymbol{\alpha}\Delta T]/2\rho\end{aligned} \tag{6}$$

where

$$\pi_0^f(T) = \Delta u^* - T\Delta s^*; \quad \Delta u^* = \overset{*}{u}{}_0^{(1)} - \overset{*}{u}{}_0^{(2)}; \quad \Delta s^* = \overset{*}{s}{}_0^{(1)} - \overset{*}{s}{}_0^{(2)}. \tag{7}$$

This function is the potential for overall stress $\boldsymbol{\sigma}$,

$$\boldsymbol{\sigma} = \rho\partial\Phi'_{eq}/\partial\varepsilon = \boldsymbol{L}[\varepsilon - z\boldsymbol{\kappa}(\boldsymbol{h}) - \boldsymbol{\alpha}\Delta T] \tag{8}$$

We shall now introduce the concept of "optimum internal arrangement". The internal arrangement is said to be optimum if the internal variables h_K are the minimizers of the free energy function (6), i.e., if the material system is in unconstrained equilibrium with respect to h_K. The necessary condition for this is

$$\frac{\partial\Phi'_{eq}}{\partial h_K} = -z\boldsymbol{\sigma}\cdot\frac{\partial\boldsymbol{\kappa}}{\partial h_K}/\rho = 0 \quad\Rightarrow\quad h_K = h_K^{eq}(\boldsymbol{\sigma}). \tag{9}$$

The formal solution $(9)_2$ of the set of algebraic Eqs. $(9)_1$ must be the function of overall stress. Hence, the equilibrium value of macroscopic eigenstrain must also be a function of $\boldsymbol{\sigma}$,

$$\boldsymbol{\kappa}(\boldsymbol{h})|_{\boldsymbol{h}=\boldsymbol{h}^{eq}} = \boldsymbol{\kappa}^{eq}(\boldsymbol{\sigma}). \tag{10}$$

Multiplying both sides of $(9)_1$ by $\partial h_K^{eq}/\partial\boldsymbol{\sigma}$ one finds the necessary condition which must be satisfied by the function $\boldsymbol{\kappa}^{eq}(\boldsymbol{\sigma})$

$$\sigma_{ij}\frac{\partial\kappa_{ij}^{eq}}{\partial\sigma_{mn}} = 0. \tag{11}$$

The condition (11) was also derived in (R *et al.*, 1992) where the function κ_{ij} was postulated to be quadratic and isotropic what precluded to reproduce the tensile-compressive asymmetry. To capture this phenomena, we shall here assume that $\boldsymbol{\kappa}^{eq}(\boldsymbol{\sigma})$ admits a potential $g^*(\boldsymbol{\sigma}) \geq 0$. Then, one can rewrite the condition (11) in the equivalent form,

$$\kappa^{eq} = \rho \frac{\partial g^*}{\partial \boldsymbol{\sigma}} \quad \Rightarrow \quad \sigma_{ij} \frac{\partial \kappa_{mn}^{eq}}{\partial \sigma_{ij}} = 0. \tag{12}$$

It is seen that (11) and (12) imply the functions $\boldsymbol{\kappa}^{eq}(\boldsymbol{\sigma})$ and $g^*(\boldsymbol{\sigma})$ to be homogeneous of order zero and one, respectively. Thus, e.g.,

$$\boldsymbol{\kappa}^{eq} \cdot \boldsymbol{\sigma} = \rho g^* \quad \text{and} \quad \sigma_{ij} g_{ijmn}^* = 0 \tag{13}$$

where $g_{ijmn}^* = \rho \partial^2 g^* / \partial \sigma_{ij} \partial \sigma_{mn}$. Moreover, since $\det \boldsymbol{g}^* = 0$ (the conclusion following from (13)) there exist one or more surfaces in κ-space along which the end of the actual "vector" of eigenstrains moves during ongoing p.t. By eliminating $\boldsymbol{\sigma}$ between (10) and (8) one can express equilibrium value of eigenstrains in terms of ε, T, and z,

$$\boldsymbol{\kappa}^{eq} = \boldsymbol{\kappa}^{eq}(Y^{T\varepsilon}), \quad Y^{T\varepsilon} = \{T, \varepsilon, z\}. \tag{14}$$

Even though derivation of the explicit formula of the type (14) in many particular cases may be cumbersome one can define the free energy function Φ of constrained phase equilibrium

$$\Phi(Y^{T\varepsilon}) = \Phi'_{eq}|_{\boldsymbol{\kappa}=\boldsymbol{\kappa}^{eq}(Y^{T\varepsilon})}$$

and associated Gibbs potential g

$$g(Y^{T\sigma}) = \{\Phi - \boldsymbol{\sigma} \cdot \boldsymbol{\varepsilon}/\rho\}_{\varepsilon=\varepsilon(Y^{T\sigma})}, \quad Y^{T\sigma} = \{T, \boldsymbol{\sigma}, z\}, \tag{15}$$

which takes the form ($\boldsymbol{M} = \boldsymbol{L}^{-1}$),

$$\begin{aligned} g(Y^{T\sigma}) &= g^A(T, \boldsymbol{\sigma}) - z\pi_0^f(T) + g^f(Y^{T\sigma}) \\ g^A &= \overset{*}{u}{}_0^{(1)} - T \overset{*}{s}{}_0^{(1)} + \bar{g}\ , \\ \bar{g} &= c_p \left[\Delta T - T \ln\left(\frac{T}{T_0}\right) \right] - (\boldsymbol{\alpha} \cdot \boldsymbol{\sigma} \Delta T/\rho) - \boldsymbol{\sigma} \cdot \boldsymbol{M}\boldsymbol{\sigma}/2\rho \\ g^f &= -zg^*(\boldsymbol{\sigma}) + z(1-z)\phi_{it}(T). \end{aligned} \tag{16}$$

The Gibbs potential of two-phase RVE being in constrained phase equilibrium is additively decomposed into three parts: the first term $g^A(T, \boldsymbol{\sigma})$ is the Gibbs free energy of thermoelastic austenite. The second term (*cf.* (7)) represents the energy of formation of martensite in absence of micro and macrostresses. It is frequently regarded as the "chemical Gibbs free energy" (*cf.*, *e.g.*, Lü *et al.*, 1990) The third term represents the mechanical energy stored in the material. The term $zg^* = z\boldsymbol{\kappa} \cdot \boldsymbol{\sigma}/\rho$ is equal to the work of macroscopic stress done on pseudoelastic strain in the course of stress assisted p.t. (it vanishes when $\boldsymbol{\sigma} = 0$), whereas the term containing ϕ_{it} represents stored energy associated with microstresses that develop during ongoing p.t. Energy and entropy differences Δu^* and Δs^* associated with formation of phases in unstressed state are much higher than the corresponding variations of energy and entropy caused by generated microstresses. Therefore, it is reasonable to assume that $\Delta u^* > \bar{u}_0$ and $\Delta s^* > \bar{s}_0$ (*cf.* (1) and (7)).

Note that the Gibbs function can be partitioned into another more familiar form (an analogy of (1))

$$g = (1 - z)g^A(T, \boldsymbol{\sigma}) + zg^M(T, \boldsymbol{\sigma}) + z(1 - z)\phi_{it}(T)$$

where g^A and g^M are Gibbs potentials of austenite and martensite, respectively, and the third term may be regarded as configurational energy. Here

$$g^M = \overset{*}{u}{}_0^{(2)} - T\overset{*}{s}{}_0^{(2)} - g^*(\boldsymbol{\sigma}) + \bar{g}(T, \boldsymbol{\sigma}).$$

where $\bar{g}$ is defined by $(16)_3$.

2.2. THERMAL EQUATIONS OF STATE

Thermal equations of state following from (16) are

$$\begin{aligned}
(17)\quad \boldsymbol{\varepsilon}(Y^{T\sigma}) &= -\rho\partial g/\partial\boldsymbol{\sigma} = \boldsymbol{M\sigma} + z\boldsymbol{\kappa} + \boldsymbol{\alpha}\Delta T, \quad \boldsymbol{\kappa} = \rho\partial g^*/\partial\boldsymbol{\sigma}\\
s(Y^{T\sigma}) &= -\partial g/\partial T = \overset{*}{s}{}_0^{(1)} - z\Delta s^* + c_p \ln\left(\frac{T}{T_0}\right) + (\boldsymbol{\alpha}\cdot\boldsymbol{\sigma}/\rho) + z(1 - z)\bar{s}_0\\
\pi^f(Y^{T\sigma}) &= -\partial g/\partial z = g^*(\boldsymbol{\sigma}) - (1 - 2z)\phi_{it} + \pi_0^f(T)
\end{aligned}$$

where s is the specific entropy of two-phase RVE, and $-\pi^f$ is the energy-conjugate force of z. Here, and what follows we neglect, for simplicity, the superscript "eq" at symbol $\boldsymbol{\kappa}$.

The first and the second laws of thermodynamics when written for infinitesimal processes of successive constrained phase equilibria take the form

$$\begin{aligned}
(18)\qquad du &= -\bar{d}\,q + \boldsymbol{\sigma}\cdot d\boldsymbol{\varepsilon}/\rho && \text{and}\\
ds + \bar{d}\,q/T &= dD/T \geq 0, && \bar{d}\,D = \pi^f dz
\end{aligned}$$

respectively. Here $u = \Phi + Ts = g + Ts + \boldsymbol{\sigma}\cdot\boldsymbol{\varepsilon}/\rho$ is the specific internal energy of RVE, dq and $\bar{d}\,D$ are the incrementals of heat exchange and energy dissipation per unit of mass, respectively. From $(18)_2$ it clearly follows that forward $(A \to M)$ p.t. can be initiated only from those states where $\pi^f \geq 0$. Likewise, the reverse p.t., $M \to A$, are admissible only at those states where $\pi^f \leq 0$. Equations (17) form the first group of constitutive equations. The complete set should contain additional kinetic relation for z. This equation is detaily discussed in (R and L, 1994) and will not be rewritten here. The general form (44) given in (R and L, 1994) also remains valid, however, the differential $d_\sigma\pi^f$ should be evaluated from the new modified Eq. $(17)_3$, i.e.,

$$(19)\qquad d_\sigma\pi^f = \pi_\sigma^f\cdot d\boldsymbol{\sigma} + \pi_T^{f\sigma}dT$$

where

$$\pi^f_\sigma = \kappa(\sigma)/\rho, \qquad \pi^{f\sigma}_T = -c^*_f/T \qquad (20)$$
$$c^*_f = T[\Delta s^* - (1 - 2z)\bar{s}_0]$$

By eliminating ds between $(17)_2$ and $(18)_2$ one obtains the incremental equation for temperature,

$$c_p dT + \bar{d}\, q = \pi^f dz - T(\boldsymbol{\alpha} \cdot d\boldsymbol{\sigma}/\rho) + c^*_f dz \qquad (21)$$

The first right-hand term represents the positive heat due to energy dissipation, the second term is the usually small heat of piezocaloric effect, whereas the last term occurring in (21) represents the apparent thermostatic heat of p.t. (*cf.* R and L, 1994).

Since the thermodynamical force π^f can be partitioned as follows

$$\pi^f(Y^{T\sigma}) = c_f(\sigma, z) - c^*_f, \qquad c_f = g^*(\sigma) + \Delta u^* - (1 - 2z)\bar{u}_0 \qquad (22)$$

the energy dissipated is partially balanced by thermostatic heat of p.t., and (21) can be rewritten in the equivalent form,

$$c_p dT + \bar{d}\, q = c_f(\sigma, z)dz - T\boldsymbol{\alpha} \cdot d\boldsymbol{\sigma}/\rho \qquad (23)$$

The quantity c_f represents the "true" latent heat of p.t. Note, that the first term occurring in $(22)_2$ when multiplied by dz represents the incremental work of pseudoelastic strain (*cf.*, (11)-(13) and $(17)_1$), i.e.,

$$\bar{d}\, W^{pe} \equiv \boldsymbol{\sigma} \cdot d\boldsymbol{\varepsilon}^{pe} = \boldsymbol{\sigma} \cdot d(\boldsymbol{\varepsilon} - \boldsymbol{\varepsilon}^e) = \boldsymbol{\sigma} \cdot d[\boldsymbol{\varepsilon} - (\boldsymbol{M}\boldsymbol{\sigma} + \boldsymbol{\alpha}\Delta T)] = \boldsymbol{\sigma} \cdot d(z\boldsymbol{\kappa}) = \rho g^* dz$$

2.3. SOME THERMOSTATIC PROPERTIES

(i) The states described by equality

$$\pi^f(Y^{T\sigma}) = 0 \qquad (24)$$

are the states of unconstrained phase equilibrium of RVE. It can be shown that when the condition

$$0 \leq \rho\phi_{it} < \frac{(\rho g^*)^2}{2\boldsymbol{\sigma} \cdot \boldsymbol{M}\boldsymbol{\sigma}} \qquad (25)$$

holds then the equilibrium is unstable. In the simplest situation, when $\boldsymbol{M}$ is isotropic and g^* depends only on deviatoric part $\bar{\boldsymbol{\sigma}}$ of stress tensor $\boldsymbol{\sigma}$, the condition (25) becomes

$$0 \leq \rho\phi_{it} < \mu\left(\frac{\rho g^*}{\sigma'}\right)^2, \qquad \sigma' = (\bar{\boldsymbol{\sigma}} \cdot \bar{\boldsymbol{\sigma}})^{1/2}, \qquad \bar{\boldsymbol{\sigma}} = dev\boldsymbol{\sigma} \qquad (26)$$

where μ is the elastic shear modulus. We found that (26) is satisfied by a number of SMA. Therefore, no real process continuously linking the unstable states is observed in such alloys. Moreover, one can conjecture that *instability of phase equilibrium is the primary origin of the observed hysteresis loops.* We shall use the condition (24) to define the critical states at which the processes of p.t. are initiated.

(ii) Consider first, the temperature-induced p.t. when $\sigma = 0$. Suppose additionally that $\phi_{it} = 0$. In this case the condition (24) (*cf.* (7) and (17)) reduces to ($g^*(0) = 0$),

$$\pi_0^f(Y^{eq}) = 0 \Longrightarrow T^{eq} = \frac{\Delta u^*}{\Delta s^*}. \tag{27}$$

Thus, forward and reverse p.t. proceed at the same constant temperature known as "equilibrium temperature" T^{eq}. Note, that $\pi_0^f(T) < 0$ for $T > T^{eq}$ since at high temperatures, the free energy of unstressed austenite is smaller than the free energy of martensite.

Return to the case when $\phi_{it} \neq 0$. The condition (24) together with $z = 0$ define the theoretical temperature M_s^0 under which $A \to M$ p.t. starts

$$\pi_0^f(M_s^0) - \phi_{it}(M_s^0) = 0 \Longleftrightarrow M_s^0 = \frac{\Delta u^* - \bar{u}_0}{\Delta s^* - \bar{s}_0}. \tag{28}$$

Likewise, combination of (24) and $z = 1$ defines the theoretical start temperature A_s^0 of the reverse ($M \to A$) p.t.,

$$\pi_0^f(A_s^0) + \phi_{it}(A_s^0) = 0 \Longleftrightarrow A_s^0 = \frac{\Delta u^* + \bar{u}_0}{\Delta s^* + \bar{s}_0}. \tag{29}$$

Hence, one arrives at the conclusion that *self-equilibriated microstresses (or their measure - the coherency energy ϕ_{it}) developed at the initial moment of nucleation of the product phase are responsible for the bifurcation of the equilibrium temperature into M_s^0 and A_s^0.*

(iii) Consider the situation when macroscopic stresses are acting, $\sigma \neq 0$. The stresses at the absolute equilibrium state $z = 0$ are those critical stresses which cause the start of isothermal stress-induced $A \to M$ p.t. Alternatively, the value of the temperature $T = M_s(\sigma)$ calculated from the condition (24) for $z = 0$ can be regarded as the critical temperature under which the stress-assisted temperature-induced p.t. begins. Thus, the condition (24) implies

$$\begin{gathered} F^{AM}(\sigma, T) \equiv g^*(\sigma) - (\Delta s^* - \bar{s}_0)(T - M_s^0) = g^*(\sigma) + \pi_0^f(T) - \phi_{it}(T) = 0 \\ M_s(\sigma) = M_s^0 + \frac{g^*(\sigma)}{\Delta s^* - \bar{s}_0} \end{gathered} \tag{30}$$

The equation $F^{AM}(\sigma, T) = 0$ describes the surface of pseudoelastic flow limits in stress space. The flows are associated with $A \to M$ p.t. This notion is analogous to the notion of initial yield limit used in the theory of plasticity. States where $F^{AM} < 0$ are states of stable thermoelastic behaviour of single austenitic phase. Likewise, the condition (24) (specified for $z = 1$) constitutes the criterion for determination of critical stresses which cause the start of stress-induced reverse $M \to A$ p.t. Alternatively, the temperature of the unconstrained equilibrium state $z = 1$ can be identified as the austenite-start temperature $A_s(\boldsymbol{\sigma})$ for stress-assisted temperature-induced p.t.,

$$(31) \quad F^{MA}(\boldsymbol{\sigma},T) \equiv g^*(\boldsymbol{\sigma}) - (\Delta s^* + \bar{s}_0)(T - A_s^0) = g^*(\boldsymbol{\sigma}) + \pi_0^f(T) + \phi_{it}(T) = 0$$

$$A_s(\boldsymbol{\sigma}) = A_s^0 + \frac{g^*(\boldsymbol{\sigma})}{\Delta s^* + \bar{s}_0}$$

On macroscopic level $M \rightarrow A$ p.t. display in the form of strain recovery phenomenon. Therefore, the surface $F^{MA}(\boldsymbol{\sigma}, T) = 0$ in stress space can be referred to as "surface of strain recovery initiation". The single phase martensite is stable for $F^{MA} > 0$. The surfaces $F^{AM} = 0$ and $F^{MA} = 0$ are the geometrical loci of two characteristic states of all outermost (bounding) hysteresis loops, i.e., loops associated with complete $A \rightarrow M$ and $M \rightarrow A$ p.t.

Since $g^* \geq 0$ one can conclude from $(30)_2$ and $(31)_2$ that the *applied macrostresses (external stresses) increase the transformation temperatures*, a feature observed experimentally for SMA behaviour.

Note, that at fixed temperature the product $(\boldsymbol{\sigma} \cdot \boldsymbol{\kappa})$ is constant for all critical states $(30)_1$ or $(31)_1$, on account of $(13)_1$. The feature (b) of the behaviour of SMA mentioned in Sec. 1 can, therefore, be easily incorporated into the present theoretical framework (*cf.* Sec. 4).

Some recently proposed thermodynamical models for three-dimensional loading cases (e.g. S and H, 1993 and B and L, 1996) do not reveal the above discussed features. It is worthwhile to mention that conditions $(30)_1$ and $(31)_1$ are 3-D counterparts of the classical Clausius-Clapeyron equation for forward and reverse phase transitions, respectively. They are not postulated "ad hoc" but conjectured from analysis of stability of unconstrained equilibrium states. The instability of equilibrium states affects also the creation of the internal hysteresis loops as discussed e.g. by M and X, 1991 for uniaxial case.

3. Isotropic solid. Generalization of R_L - models

The generalized theoretical framework discussed in Sec. 2 will now be used to get the simplest version of the theory that incorporate all effects listed in Sec.1.

To this end adopt the following simplifications:

- the behaviour of two-phase RVE is isotropic,
- macroscopic eigenstrain $\boldsymbol{\kappa}$ is independent of hydrostatic pressure.

These imply that the potential g^* is at most isotropic function of stress deviator $\bar{\boldsymbol{\sigma}}$. Taking into account that g^* is homogeneous function of order one, we conclude that its most general representation (in the class of regular functions in a domain of $\bar{\boldsymbol{\sigma}} \neq 0$) may be written in the form,

$$(32) \qquad \rho g^*(\bar{\boldsymbol{\sigma}}) = \eta\sigma' f(y); \quad y = \sqrt{6} tr \boldsymbol{N}^3 = \frac{3\sqrt{6}J_3^\sigma}{(\sigma')^3}; \quad \boldsymbol{N} = \frac{\bar{\boldsymbol{\sigma}}}{\sigma'}$$

where

$$(33) \qquad (\sigma')^2 = tr\bar{\boldsymbol{\sigma}}^2; \qquad J_3^\sigma = det\bar{\boldsymbol{\sigma}} = \frac{1}{3} tr\bar{\boldsymbol{\sigma}}^3$$

η is a constant and $f(y)$ is positive dimensionless scale (or shape) function which is stipulated to satisfy two mathematical conditions,

$$(34) \qquad f = 1 \qquad \text{and} \qquad \frac{df}{dy} = 0 \qquad \text{for} \quad y = 0$$

The specific numeric factor occurring in the definition of y normalizes this variable such that $|y| \leq 1$ for all stress states. When $f = 1$ for all y then the theory reduces to the one given in (R *et al.*, 1992).

The strain-stress relations now become

$$(35) \qquad \begin{aligned} &tr\boldsymbol{\varepsilon} = \frac{tr\boldsymbol{\sigma}}{3K} + 3\alpha(T - T_0); \quad \boldsymbol{\varepsilon}' = dev\boldsymbol{\varepsilon} = \frac{\bar{\boldsymbol{\sigma}}}{2\mu} + z\boldsymbol{\kappa} \\ &\boldsymbol{\kappa} = \bar{\boldsymbol{\kappa}} + \bar{\bar{\boldsymbol{\kappa}}} \\ &\bar{\boldsymbol{\kappa}} = \eta f(y)\boldsymbol{N}; \qquad \bar{\bar{\boldsymbol{\kappa}}} = 3\eta\frac{df}{dy}[\sqrt{6}(\boldsymbol{N}^2 - \mathbf{1}/3) - y\boldsymbol{N}] \end{aligned}$$

where K and μ are bulk and shear moduli, respectively, and α is the coefficient of linear thermal expansion. The eigenstrain $\boldsymbol{\kappa}$ is split additively into two parts which are mutually orthogonal in the sense that $tr(\bar{\boldsymbol{\kappa}}\,\bar{\bar{\boldsymbol{\kappa}}}) = 0$, what follows from the fact that $tr(\bar{\bar{\boldsymbol{\kappa}}}\boldsymbol{N}) = 0$. The part $\bar{\bar{\boldsymbol{\kappa}}}$ did not appear in previous works (R *et al.*, 1992) and (R and L, 1994).

The equivalent eigenstrain $\bar{\gamma}$ is defined as follows,

$$(36) \qquad \bar{\gamma}(y) = \left[\frac{2}{3}tr\boldsymbol{\kappa}^2\right]^{1/2} = \gamma\left[f^2 + 9\left(\frac{df}{dy}\right)^2(1 - y^2)\right]^{1/2}; \quad \gamma = \eta\sqrt{\frac{2}{3}}$$

The new constant γ introduced here can be identified as equivalent eigenstrain in the situation when $y = 0$, e.g., in pure shear (*cf.* Sec. 4.2), on account of the assumption $(34)_2$. It is seen that pseudoelastic strain is independent of the magnitude of stress deviator and varies only with variations of its direction $\boldsymbol{N}$ in the stress deviator space. Since $\text{tr}(\boldsymbol{N}) = 0$ and $\text{tr}(\boldsymbol{N}^2) = 1$, the tensor $\boldsymbol{N}$ has at most 4 independent components. They can be regarded as parameters when writing the parametric form of a surface in 5-dimensional space of second order tensor deviators. Thus, e.g., Eqs. $(35)_{2,3}$ describe a surface (in $\boldsymbol{\kappa}$-space) which is the geometrical loci of all admissible values of eigenstrain. The last thermal equation of state, i.e., the expression for thermodynamical force π^f now become

$$(37) \qquad \pi^f = \frac{\eta}{\rho}\sigma' f(y) - (1 - 2z)\phi_{it} + \pi_0^f(T)$$

The parametric forms of equations of surfaces $F^{AM}(\boldsymbol{\sigma}, T) = 0$ and $F^{MA}(\boldsymbol{\sigma}, T) = 0$ (*cf.* (30) and (31)) are

$$(38) \qquad \bar{\boldsymbol{\sigma}} = \sqrt{\frac{2}{3}}\sigma^{AM}(y, T)\boldsymbol{N} \qquad \text{and} \qquad \bar{\boldsymbol{\sigma}} = \sqrt{\frac{2}{3}}\sigma^{MA}(y, T)\boldsymbol{N}$$

$$\sigma^{AM}(y, T) = \frac{\rho(\Delta s^* - \bar{s}_0)(T - M_s^0)}{\gamma f(y)} > 0;$$

$$\sigma^{MA}(y, T) = \frac{\rho(\Delta s^* + \bar{s}_0)(T - A_s^0)}{\gamma f(y)} > 0$$

Here, σ^{AM} and σ^{MA} are the critical values of the effective stress defined by

$$(39) \qquad \bar{\sigma} = \sqrt{\frac{3}{2}}\sigma' = \left(\frac{3}{2}\bar{\boldsymbol{\sigma}} \cdot \bar{\boldsymbol{\sigma}}\right)^{1/2}$$

They are linear functions of T (*cf.* property (b), Sec. 1). The temperature sensitivity of pseudoelastic flow and recovery limits measured by $\partial\sigma^{AM}/\partial T$ and $\partial\sigma^{MA}/\partial T$ depend on $\boldsymbol{N}$ through dependence of f on y. In Sec. 4 we show that the observed experimental facts mentioned in Sec. 1 impose additional restriction upon admissible function $f(y)$.

The width of an outermost hysteresis loop (measured at fixed T and $\boldsymbol{N}$) on $\bar{\gamma} - \bar{\sigma}$ plane is defined by

$$\Delta\sigma(y,T) = \sigma^{AM}(y,T) - \sigma^{MA}(y,T).$$

Calculating $\Delta\sigma$ with the aid of (37) and multiplying the result by $\bar{\gamma}(y)$ one finds,

$$(40) \qquad \Delta\sigma(y,T)\bar{\gamma}(y) = 2\rho\phi_{it}(T)\left[1 + 9\left(\frac{dlnf}{dy}\right)^2(1-y^2)\right]^{1/2}$$

Thus, the product of the width of a loop and the equivalent eigenstrain is not completely determined by the coherency energy ϕ_{it}, unless $y = 1$ or $y = 0$ (the latter value follows from the heuristic assumption $(34)_2$).

4. Simple tension-compression. Pure shear

4.1. SIMPLE TENSION-COMPRESSION

(i) For uniaxial stress state

$$(41) \qquad \sigma_{ij} = \sigma_{11}\delta_{i1}\delta_{j1}; \quad \bar{\sigma}_{ij} = \frac{2}{3}\sigma_{11}U_{ij}; \quad U_{ij} = \delta_{i1}\delta_{j1} - 0.5(\delta_{i2}\delta_{j2} + \delta_{i3}\delta_{j3})$$

one finds (*cf.* (32)) $\sigma' = |\sigma_{11}|\sqrt{\frac{2}{3}}$, $J_3^{\sigma} = 2 \cdot \sigma_{11}^3/27$,

$$(42) \qquad \boldsymbol{N} = \pm\sqrt{\frac{2}{3}}\boldsymbol{U}, \quad y = \pm 1$$

where the upper and lower sign correspond to the tension and compression, respectively. Hence, (*cf.* (35-36)) $\bar{\bar{\boldsymbol{\kappa}}} = 0$ and

$$(43) \qquad \rho g^* = |\sigma_{11}| \cdot \bar{\gamma}(\pm 1), \quad \bar{\gamma}(\pm 1) = \gamma \cdot f(\pm 1), \quad \boldsymbol{\kappa} = \pm\bar{\gamma}(\pm 1) \cdot \boldsymbol{U}$$

Moreover, (*cf.* $(37)_1$), the critical values of σ_{11} are $\sigma_{11} = \pm\sigma^{AM}(\pm 1, T)$ and $\sigma_{11} = \pm\sigma^{MA}(\pm 1, T)$ for uniaxial pseudoelastic flow and recovery, respectively, where (*cf.* $(37)_2$)

$$(44) \qquad \begin{aligned} \bar{\gamma}(\pm 1) \cdot \sigma^{AM}(\pm 1, T) &= \rho(\Delta s^* - \bar{s}_0)(T - M_s^0) \\ \bar{\gamma}(\pm 1) \cdot \sigma^{MA}(\pm 1, T) &= \rho(\Delta s^* + \bar{s}_0)(T - A_s^0) \end{aligned}$$

such that (*cf.* (40)),

$$(45) \qquad \bar{\gamma}(\pm 1) \cdot \Delta\sigma(\pm 1, T) = 2\rho\phi_{it}(T)$$

The uniaxial stress-strain relation and the expression for thermodynamic force π^f take the form (E is the Young modulus) - *cf.* (35) and (37),

$$\varepsilon_{11} = (\sigma_{11}/E) + \alpha(T - T_0) \pm \bar{\gamma}(\pm 1)z \tag{46}$$

and

$$\pi^f = \bar{\gamma}(\pm 1) \cdot (|\sigma_{11}|/\rho) - (1 - 2z)\phi_{it} + \pi_0^f(T) \tag{47}$$

It is seen that in this case the equivalent eigenstrain can be identified as pseudoelastic strain amplitude.

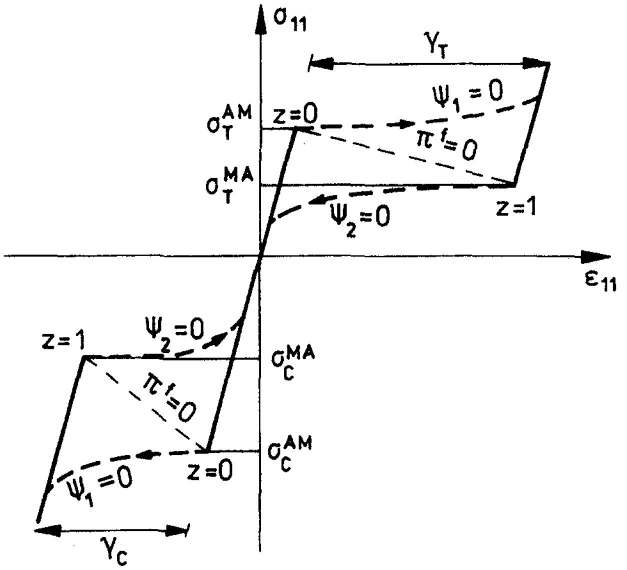

Fig. 1. – Illustration of the isothermal relationship between uniaxial stress and strain (pseudoelasticity: $T > A_f^0$).

(ii) The states of absolute equilibrium in uniaxial stress state for fixed T (thermal expansion is neglected) are illustrated in Figure 1. The straight line segment containing the origin of the coordinate system illustrates the elastic behaviour of stable austenite. The other two ascending straight lines show the behaviour of stable martensite. The geometrical loci of unstable two-phase equilibrium states are the descending straight line segments $\pi^f = 0$. Figure 2 illustrates the dependence of pseudoelastic flow and recovery limits on the temperature. The straight line containing M_s^0 can also be regarded as geometrical loci of martensite-start temperatures $T = M_s(\sigma_{11})$. In such case T is treated as dependent variable. Likewise, straight lines containing A_s^0 illustrate critical temperatures $T = A_s(\sigma_{11})$ of stress-assisted reverse $M \rightarrow A$ p.t. In Figures 1 and 2, the following abbreviated notation is used

$$\gamma_T = \bar{\gamma}(+1), \quad \sigma_T^{AM} = \sigma^{AM}(+1, T), \quad \sigma_T^{MA} = \sigma^{MA}(+1, T)$$

$$\gamma_C = \bar{\gamma}(-1), \quad \sigma_C^{AM} = -\sigma^{AM}(-1, T) < 0, \quad \sigma_C^{MA} = -\sigma^{MA}(-1, T) < 0$$

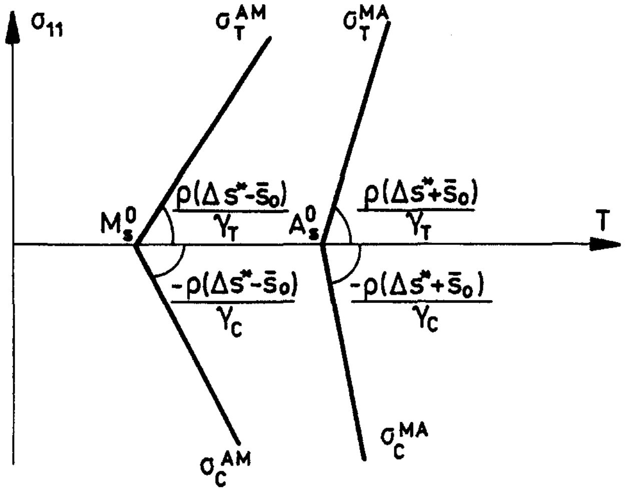

Fig. 2. – Illustration of variation of the critical stresses with temperature for forward ($A \rightarrow M$) and reverse ($M \rightarrow A$) p.t. in simple tension-compression.

(iii) The experimental observations confirm the predictions of thermodynamic theory. The Eq. (44) shows that the feature of the behaviour of SMA observed by [O and F, 1996] (equality of the products of σ^{AM} and $\bar{\gamma}$ for tension and compression - *cf.* the property (b)-Sec.1) is *the thermodynamical property.* On the other hand, for a number of SMA (*cf.* V and L, 1991 and O and F, 1996) $\sigma^{AM}(+1,T) < \sigma^{AM}(-1,T)$. When this fact is combined with (44) the latter equation implies $\bar{\gamma}(+1) > \bar{\gamma}(-1)$ (the complement of the property (b)-Sec.1). Hence the observations (a)-(b) impose the following restriction on the function $f(y)$ (*cf.* $(43)_1$) occurring in the definition of the potential g^* (*cf.* $(32)_1$)

$$f(+1) > f(-1) \tag{48}$$

When the mathematical property (48) holds then the features (c) and (d) listed in Sec.1 follow directly from the thermodynamical properties $(44)_1$ and (45),

$$\frac{\partial\sigma^{AM}}{\partial T}(-1,T) > \frac{\partial\sigma^{AM}}{\partial T}(+1,T); \quad \Delta\sigma(-1,T) > \Delta\sigma(+1,T)$$

Thus, the inequality (48) is the only condition which is necessary to include the experimental facts (a)-(d) (Sec. 1) into the theory. Moreover, when (48) is satisfied the developed theory suggests that the similar properties concern also the reverse p.t.,

$$\frac{\partial\sigma^{MA}}{\partial T}(-1,T) > \frac{\partial\sigma^{MA}}{\partial T}(+1,T); \quad \sigma^{MA}(-1,T) > \sigma^{MA}(+1,T)$$

4.2. PURE SHEAR

For pure shear

$$\sigma_{ik} = \sigma_{12}S_{ik} = \bar{\sigma}_{ik}, \qquad S_{ij} = (\delta_{i1}\delta_{j2} + \delta_{i2}\delta_{j1}) \tag{49}$$

one finds $\sigma' = \sqrt{2}|\sigma_{12}|$, $J_3^\sigma = 0$ and

$$N = \frac{\sqrt{2}}{2}sgn(\sigma_{12})S, \qquad y = 0 \qquad f(0) = 1. \tag{50}$$

Hence,

$$(51)\qquad \rho g^* = \sqrt{3}\gamma|\sigma_{12}|, \qquad \bar{\gamma}(y)\,|_{y=0} = \gamma = \text{const}, \quad \boldsymbol{\kappa} = \bar{\boldsymbol{\kappa}} = \frac{\sqrt{3}}{2}\gamma(sgn\sigma_{12})\boldsymbol{S}$$

The critical values of σ_{12} are $|\sigma_{12}| = \sigma^{AM}(0,T)/\sqrt{3}$ and $|\sigma_{12}| = \sigma^{MA}(0,T)/\sqrt{3}$ for pseudoelastic flow and recovery, respectively, where

$$(52)\qquad \begin{aligned} \sigma^{AM}(0,T) &= \rho(\Delta s^* - \bar{s}_0)(T - M_s^0)/\gamma; \\ \sigma^{MA}(0,T) &= \rho(\Delta s^* + \bar{s}_0)(T - A_s^0)/\gamma \end{aligned}$$

They are not influenced by shearing direction. Thus, the characteristic feature (e) of pseudoelastic behaviour in pure shear, mentioned in Sec. 1, is incorporated in the present theory.

The ratios ω_σ of pseudoelastic limits in pure shear and simple tension (compression) are

$$(53)\qquad \omega_\sigma \equiv \frac{\sigma^{AM}(0,T)/\sqrt{3}}{\sigma^{AM}(\pm 1,T)} = \frac{\sigma^{MA}(0,T)/\sqrt{3}}{\sigma^{MA}(\pm 1,T)} = f(\pm 1)/\sqrt{3}.$$

They are independent of T unless scale function f is temperature-dependent. The stress-strain relation and the expression for π^f now become (*cf.* (35), (37))

$$(54)\qquad \begin{aligned} \varepsilon_{12} &= \frac{\sigma_{12}}{2\mu} + \frac{\sqrt{3}}{2}\gamma[sgn(\sigma_{12})]z \\ \pi^f &= \frac{\sqrt{3}}{2}\gamma|(\sigma_{12})| - (1-2z)\phi_{it} + \pi_0^f \end{aligned}$$

Thus, the constant γ is proportional to the amplitude γ_s of pseudoelasticity in pure shear

$$(55)\qquad \gamma_s = \sqrt{3}\gamma/2$$

Moreover, there is definite relation between ω_σ and ratios of pseudoelastic amplitudes in tension (compression) and pure shear

$$(56)\qquad \omega_\sigma = \frac{1}{2}\frac{\bar{\gamma}(\pm 1)}{\gamma_s} = f(\pm 1)/\sqrt{3}$$

and account of $(43)_2$. Note, however, that the conclusions presented in this Section are the consequences of the heuristic assumption $(34)_2$ which, if necessary, can be modified in further development of the thermodynamic theory.

4.3. EQUATION OF BOUNDING HYSTERESIS LOOP

The hysteresis loop associated with complete forward and reverse p.t. is refereed to as "bounding" loop. Two of such loops (for tension and compression) are illustrated in Figure 1. The active pseudoelastic flow $(dz > 0)$ associated with complete $(z = 0 \rightarrow z = 1)$ forward p.t. $(A \rightarrow M)$ proceeds along the line segment $\psi_1 = 0$, whereas the active pseudoelastic strain recovery accompanied by complete reverse p.t. ($M \rightarrow A$, $dz < 0$) occurs along the segment $\psi_2 = 0$. According to the general equation of transformation kinetics discussed in [R and L, 1994] ψ_α are defined by

$$\begin{aligned} \psi_1 &= (\pi^f/2\bar{u}_0)^{m_1} - p_1 z + r_1 \ln(1-z) \\ \psi_2 &= (-\pi^f/2\bar{u}_0)^{m_2} - p_2(1-z) + r_2 \ln(z) \end{aligned} \tag{57}$$

where $m_\alpha \geq 1$, p_α and r_α ($\alpha = 1, 2$) are non-negative phenomenological constants. Using (57) and eliminating π^f from the set of algebraic equations $\psi_\alpha = 0$ and (47) one finds the following relations between uniaxial stress and z

$$|\sigma_{11}| = \sigma^{AM}(\pm 1, T) + \frac{2\rho\bar{u}_0}{\bar{\gamma}(\pm 1)}[p_1 z - r_1 \ln(1-z)]^{1/m_1} - \frac{2\rho\phi_{it}}{\bar{\gamma}(\pm 1)} z \tag{58}$$

for the segment $\psi_1 = 0$ (associated with $A \rightarrow M$ p.t.) of bounding hysteresis loop, and

$$|\sigma_{11}| = \sigma^{MA}(\pm 1, T) - \frac{2\rho\bar{u}_0}{\bar{\gamma}(\pm 1)}[p_2(1-z) - r_2 \ln(z)]^{1/m_2} + \frac{2\rho\phi_{it}}{\bar{\gamma}(\pm 1)}(1-z) \tag{59}$$

for the strain recovery segment ($\psi_2 = 0$) of the bounding loop, where σ^{AM} and σ^{MA} are defined by (44). The set of algebraic Eqs. (46) and (58), (59) constitutes the parametric form (z is regarded as parameter, $0 < z < 1$) of the equations of the bounding hysteresis loops on $\sigma_{11} - \varepsilon_{11}$ plane for simple tension and compression. Similar equations can be derived for pure shear. They will not be discussed here.

4.4. DETERMINATION OF CONSTANTS FOR *NiTi* ALLOY

To identify the physical constants and to have a view upon the validity of the predictions of the theory we used the experimental data reported in [O and F, 1996] for equatomic *NiTi* alloy supplied by Memometal Industry. The basic elastic constants for this alloy are given in Table I. To identify the thermostatic constants $\bar{s}_0, \Delta s^*, \Delta u^*$ and $\bar{u}_0$ we used the measured $\sigma_{11} - \varepsilon_{11}$ hysteresis loops (for simple tension and compression) presented in (O and F, 1996) for the temperature $T_1 = 333K$. A number of experimental points are

TABLE I.

Properties	Value
ρ $[kg/m^3]$	6500
E $[MPa]$	55000
ν (Poisson ratio)	0.29
Δu^* $[J/kg]$	23800
$\bar{u}_0$ $[J/kg]$	1000
Δs^* $[J/kgK]$	80
$\bar{s}_0$ $[J/kgK]$	0
γ	0.061
$f(+1)$	1.05
$f(-1)$	0.744

reproduced in Figure 3 and denoted by special signs × and □. The loops were regarded as bounding one i.e., associated with the complete forward and reverse p.t. Directly from the presented curves we estimated pseudoelastic amplitudes $\bar{\gamma}(+1)$ and $\bar{\gamma}(-1)$, as well as pseudoelastic flow and recovery limits $\sigma^{AM}(+1,T_1)$ and $\sigma^{MA}(+1,T_1)$ for *simple tension.*

$$\begin{gathered}\bar{\gamma}(+1) = 0.064; \quad \bar{\gamma}(-1) = 0.0454; \\ \sigma^{AM}(+1,T_1) = 390MPa; \quad \sigma^{\mathrm{MPa}}(+1,T_1) = 187 \text{ MPa}\end{gathered} \tag{60}$$

The estimation of pseudoelastic amplitudes made by [O and F, 1996] brought different values since they were identified as maximum recovery strains obtained after simple tension performed at $T_2 = 293\ K$, i.e., out of the pseudoelastic temperature range $(T_2 < A_f = 329\ K)$. However, the ratio ω_γ of pseudoelastic amplitudes in both cases are the same

$$\omega_\gamma = \bar{\gamma}(-1)/\bar{\gamma}(+1) \approx 0.71 \tag{61}$$

We also used the experimental data concerning $\sigma_{11} - T$ relation *for tension* presented in [O and F, 1996] and shown in Figure 4. The experimental points represents the critical values $\sigma^{AM}(\pm 1, T)$ of uniaxial stress for different temperatures. They were estimated from $\sigma_{11} - \varepsilon_{11}$ curves by [O & F, 1996]. We have approximated data for tension by straight line passing through point $(\sigma_{11} = 390 \text{ MPa}, T = T_1 = 333\ K)$ and extrapolated it to $\sigma_{11} = 0$ and $T = M_s^0$. The theoretical value M_s^0 was found to be $M_s^0 = 285\ K$ - five degree higher than measured by DSC technique (*cf.* O and F, 1996). Furthermore, we have neglected interfacial entropy $\bar{s}_0 = 0$. The data (60) and values of M_s^0 and $\bar{s}_0 = 0$ are sufficient for determination of $\Delta s^*, \Delta u^*$ and $\bar{u}_0$. From the set of Eqs (44), $(28)_2$ and $(29)_2$ one finds

$$\begin{aligned} A_s^0 &= T_1 - (T_1 - M_s^0)\sigma^{MA}(+1,T_1)/\sigma^{AM}(+1,T_1); \\ \rho\Delta s^* &= \frac{\bar{\gamma}(+1)\sigma^{AM}(+1,T_1)}{T_1 - M_s^0} \\ \Delta u^* &= \frac{1}{2}\Delta s^*(M_s^0 + A_s^0); \quad \bar{u}_0 = \frac{1}{2}\Delta s^*(A_s^0 - M_s^0) \end{aligned} \tag{62}$$

The constants $\Delta s^*, \Delta u^*$ and $\bar{u}_0$ given in Table 1 were calculated from Eqs. (62). The theoretical value of austenistic-start temperature A_s^0 was found to be 310 K - ten degree higher than the one measured by application of DSC technique. The remaining thermostatic constant γ was estimated from the results of cyclic shear test presented in the paper of (O and F, 1996) and reproduced in Figure 6. We have estimated pseudoelasticity limit in shear to be $\sigma^{AM}(0,T_1)/\sqrt{3} = 236$ MPa. Then, using data (60) for tension we found the value of the ratio ω_σ (*cf.* (53)), $\omega_\sigma(+1) = 0.605$. The value of γ was calculated with use of (55-56), $\gamma = \bar{\gamma}(+1)/[\sqrt{3}\omega_\sigma(+1)] \cong 0.061$. However, this value is uncertain and can not be verified because of we have no information about the maximum pseudoelastic strain generated during the first cycle.

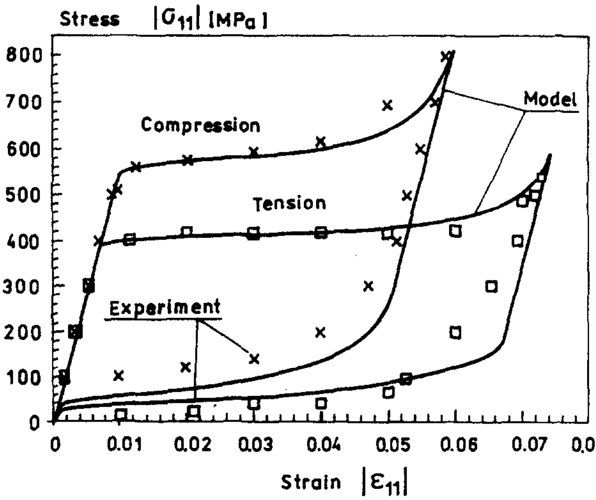

Fig. 3. – Pseudoelastic tension-compression curve of NiTi, $T = 333$ K (experimental points - after [O and F, 1996]).

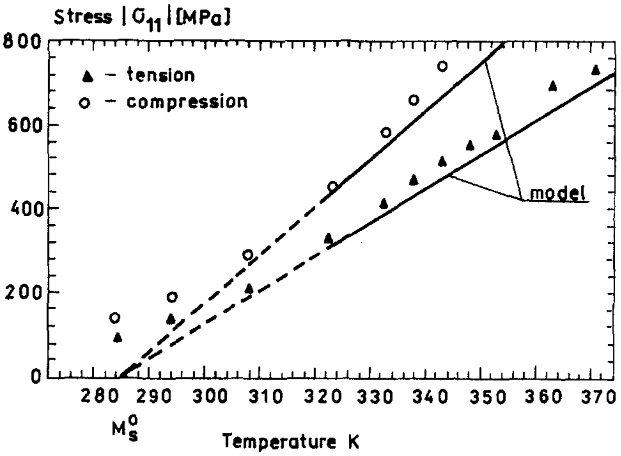

Fig. 4. – Variation of the limit of pseudoelastic flow σ^{AM} with T in simple tension-compression of NiTi (experimental points - after [O and F, 1996]).

Having known all thermoelastic constants, one *can predict* other properties of the alloy. For example, limits of pseudoelastic flow and strain recovery in compression and pure shear can be calculated from (44) and (52). They are

$$\sigma^{AM}(-1,T_1) = 549 \text{ MPa}; \quad \sigma^{MA}(-1,T_1) = 263 \text{ MPa (compression)} \tag{63}$$
$$\sigma^{MA}(0,T_1)/\sqrt{3} = 113 \text{ MPa (shear)}$$

The predicted temperature-sensitivity of pseudoelastic limits are

$$\frac{\partial\sigma^{AM}(+1,T_1)}{\partial T} = 8.125 \text{ MPa}/K; \quad \frac{\partial\sigma^{AM}(-1,T_1)}{\partial T} = 11.45 \text{ MPa}/K \tag{64}$$

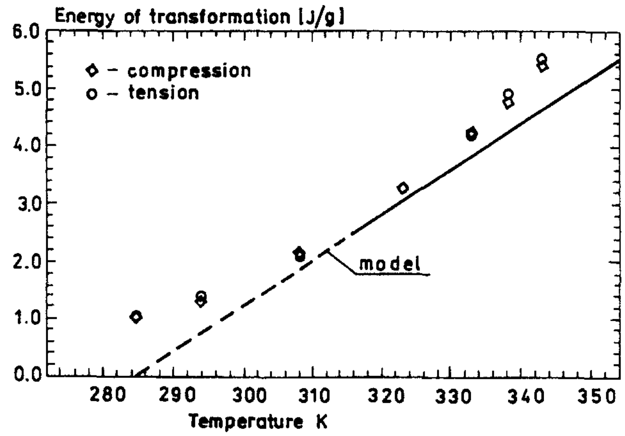

Fig. 5. – Variation of the transformation energy with T in simple tension-compression of NiTi (experimental points - after [O and F, 1996] with modified energy-axis scale).

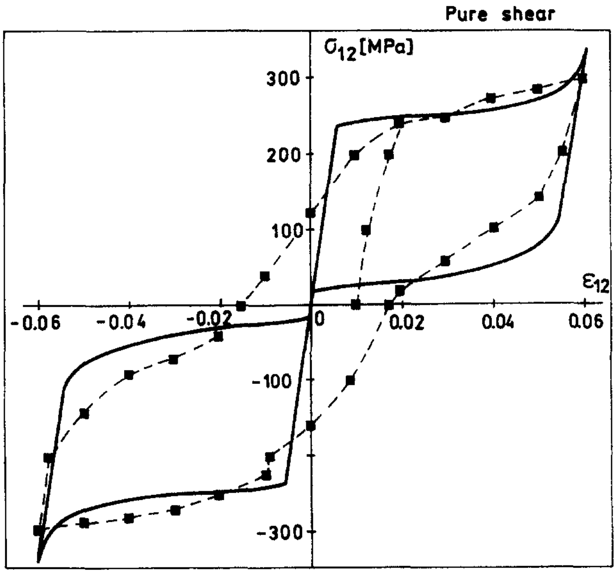

Fig. 6. – Predicted hysteresis loop in pure shear for NiTi at $T = 333$ K (individual points represent results of cyclic shear test discussed by [O and F, 1996]).

These coefficients define the slopes of theoretical straight lines presented in Figure 4. The comparisons of theoretical and experimental results (*cf.* Figs 3, 4 and 6) show that predicted values (63-64) are reasonable.

The experimental points reproduced in Figure 5 make evidence that energies of p.t. represented by product $\bar{\gamma}\sigma^{AM}$ are the same for tension and compression at every temperature. When marking this points we multiplied the energy-axis scale by factor $\omega_\gamma = 0.71$ (*cf.* (61)) in order to account for the fact that our estimation of pseudoelastic amplitudes are different from those given in (O and F, 1996). The discrepancies between experimental points and points of theoretical straight line observed in Figure 5 are acceptable. One of the reasons of their occurrence is that our estimation of σ^{AM}, $\sigma^{AM}(+1, T_1) = 390$ MPa, is different from the one made by (O and F, 1996) ($\sigma^{AM}(+1, T_1) \cong 412$ MPa).

To identify the phenomenological constants given in Table II we have chosen a few characteristic points on experimental *tension curve* and used formula (58-59). The comparison of predicted hysteresis loop for compression with experiments is shown in Figure 3. In Figure 6, the theoretical hysteresis loop for pure shear is shown on the background of experimental points representing the results of cyclic shear test (*cf.* O and F, 1996). Since we do not know the behaviour of a specimen during the first cycle, the latter comparison demonstrates only that the characteristic parameters of the experimental and theoretical loops are of qualitative agreement.

TABLE II.

Constant	Value
Flow ($\alpha = 1$)	
m_1	1.25
p_1	0.64
r_1	0.35
Recovery ($\alpha = 2$)	
m_2	1.7
p_2	2.42
r_2	0.063

5. Discussion

In this paper, the thermodynamic theory of pseudoelastic behaviour of SMA is generalized to account for new observed effects, in particular, the type of Strength Differential Effect in SMA, *i.e.*, occurrence of large differences between hysteresis loops measured in tension and compression. The thermodynamic description used in this paper is simplified since no notions of discontinuous fields of microstrains and microstresses are employed. Instead, the piecewise uniform fields are considered and an extra term - coherency energy is added to the free energy function in order to account for the energy concentrated near the moveable phase boundaries. In general, the coherency energy terms Δu^* and $\Delta s^* T$, as well as phase eigenstrain, depend upon microstructure changes. Here only the latter dependence is accounted for (in general terms). Under this assumption, it was shown that equilibrium values of macroscopic eigenstrain κ^{eq} is homogeneous function of stress of order zero, provided that it admits the potential. In effect, there exists at least one constraint relation which actual equilibrium eigenstrain must satisfy. During actual process of straining, a two-phase macroscopic material element is not in a state of phase equilibrium because of such states are unstable. This fact was utilized to define the initial pseudoelastic flow limit and the strain recovery limit. As a consequence, the stress limits are known when the form of thermodynamic potential is specified. The critical stresses are thus the thermodynamical properties of SMA. They are linear function of temperature and depend on the direction N of loading in the stress space.

The Gibbs free energy function discussed here for isotropic solids employs only five new constants and one scale function f (of single variable) in addition to the constants used in usual infinitesimal theory of thermoelasticity. Two values of the function f (corresponding to tension and compression) and all new constants are found for NiTi alloy. Moreover, it has been shown that all features of behaviour of SMA discussed by (O and F, 1996) are incorporated into the developed theory. The comparison of experimental and theoretical results presented here show good agreement.

While the present paper was under process of reviewing we have been acquinted with the paper (Jacobus *et. al.*, 1996) where new experimental results for NiTi alloy under triaxial stress state are reported. Although some of the statements (concerning the possibility of theoretical description of the reported results) present in (J *et al.*, 1996) are questionable, the work is probably the first where the effect of hydrostatic stress upon behaviour of NiTi are systematically investigated. The provided results show that pseudoelastic flow limits under uniaxial compression and triaxial compression (in both cases $y = -1$; *cf.* Eq. (32)) differ by about 15%, whereas under zero hydrostatic stress and uniaxial tension (in both cases $y = 1$) the difference is negligible. Thus, the higher is the hydrostatic pressure the more pronounced is its influence upon the pseudoelastic flow limit. Within the present approach this effect could be accounted for by assuming that, at equilibrium, not only the potential g^* but also the configurational energy ϕ_{it} and the chemical energy π_0^f depend on hydrostatic stress $\text{tr}\sigma/3$.

Acknowledgements. – One of us (BR) gratefully acknowledges the financial support of the Polish National Committee of Sciences (KBN project No. 3P40403507).

REFERENCES

BOYD J.G., LAGOUDAS D.C., 1996, A thermodynamical constitutive model for shape memory materials. Part I. The monolithic shape memory alloy, *Int. J. Plasticity*, **12**, 6, 805-842.

HUO Y., MÜLLER I., 1993, Nonequilibrium thermodynamics of pseudoelasticity, *Continuum Mech. Thermodyn.*, **5**, 163-204.

JESSE LIM T., MCDOWELL D.L., 1995, Path dependence of shape memory alloys during cycling loading, *J. of Int. mat. Systems and Structures*, **6**, 817-839.

JACOBUS K., SEHITOGLU H., BALZER M., 1996, Effect of stress state on the stress-induced martensitic transformation in polycrystalline Ni-Ti alloy, *Metallurgical and Materials Transations A*, **27A**, 3066-3073.

LECLERCQ S., LEXCELLENT C., GELIN J.C., 1996, A finite element calculation of devices made of shape memory alloys, *Journal de Physique IV, Colloque C1, supplément au Journal de Physique III*, v. 6, 225-234.

LECLERCQ S., LEXCELLENT C., 1996, A general macroscopic description of the thermomechanical behaviour of shape memory alloys, *J. Mech. Phys. Solids*, **44**, 6, 953-980.

LÜ L., AERNOUDT E., WOLLANTS P., DELAEY L., 1990, Simulation of transformation hysteresis, *Z. Metallkole*, Bd 81, H.9, 613-622.

MÜLLER I., 1989, On the size of the hysteresis in pseudoelasticity, *Continuum Mech. Thermodyn.*, **1**, 125-142.

MÜLLER I., XU H., 1991, On the pseudoelastic hysteresis, *Acta Metall. Mater.*, **39**, 263-271.

ORGEAS L., FAVIER D., 1996, Non symmetric tension-compression behavior of Ni Ti alloy, *J. de Phys. IV*, C8, 605-610.

RANIECKI B., LEXCELLENT C., 1994, R_L-models of pseudelasticity and their specification for some shape memory solids, *Eur. J. Mech. A /Solids*, **12**, 1, 21-50.

RANIECKI B., LEXCELLENT C., TANAKA K., 1992, Thermodynamic models of pseudoelastic behaviour of shape memory alloys, *Arch. Mech.*, **44**, 3, 261-284.

ROGUEDA C., LEXCELLENT C., BOCHER L., 1996, Experimental study of pseudoelastic behaviour of CuZnAl polycrystalline shape memory alloy under tension - torsion proportional and non-proportionalloading tests, *Arch. Mech.* **48**, 6, 1025-1045.

ROUMAGNAC P., 1993, Etude du comportement en phase martensitique et de l'effet mémoire simple d'alliages à mémoire de forme Nickel-Titane en fonction du mode de sollicitation, P.D. Thesis, UT Compiègne.

SITTNER P., TOKUDA M., 1994, Thermoelastic martensitic transformation under combined stress-simulation and experiments, Proc. of 15th RisøInternational Symposium on Material Science: Numerical Predictions of Deformation Processes and the Behaviour of Real Materials, Ed. S.I. Andersen *et al.*, RisøNational Laboratory, Roskilde, Denmark, 537-544.

SUN Q.P., HWANG K.Ch., 1993, Micromechanic modelling for the constitutive behaviour of polycrystalline shape memory alloys, Part I and II, *J. Mech. Phys. Solids*, **41**, 1. 1-17 and 19-33.

VACHER P., LEXCELLENT C., 1991, Study of pseudoelastic behaviour of polycrystalline shape memory alloys by resistivity measurements and acoustic emission, Proceedings of ICM VI, Kyoto, Vol. 3, 231-236.

ŹIÓŁKOWSKI A., 1993, Theoretical analysis of efficiency of shape memory alloy heat engines (based on constitutive models of pseudoelasticity). *Mechanics of Materials* **16**, 365-377.

ŹIÓŁKOWSKI A., RANIECKI B., 1996, FEM - Analysis of the one-dimensional coupled thermomechanical problem of TiNi SMA, *Journal de Physique IV, Colloque C1, supplément au Journal de Physique III*, v. 6, 395-403.

(Manuscript received March 25, 1997;
revised December 15, 1997.)